Engineered Science
DOI: https://dx.doi.org/10.30919/es1222

Time-Shifted Gramian Angular Field and Recursive Plot Convolutional Neural Network to Adapt Solar Cell Dataset Overfitting in Hybrid Power Generation

Suherman Suherman,[1,*] Ali Hanafiah Rambe,[1] Nismah Panjaitan,[2] and Ahmed Saeed Alfakeeh[3]

Abstract

This Solar cell power generation has been employed widely. Battery storage becomes an important part of ensuring output availability. However, battery prices and technologies are costly. Hybrid generation for daylight supply becomes one of the solutions. This paper proposed hybrid solar cell-diesel power generation. Diesel power generation should maintain overall power requirements to fulfill demand. Since irradiation changes relative to the sun's position on the earth, solar cell power output varies overtime. As the solar cell output changes overtime, the diesel power generation should be determined. The differences between the predicted solar power and the energy demand determine the energy amount that the diesel generator should provide. In order to provide prediction, convolutional neural networks utilizing multilayer perceptron with hyper-parameter optimizations and statistics transformation, as well as data transformation, are employed. However, solar cell data is highly overfitted. The folded and time-shifted gramian angular field and recursive plot are then proposed. As a result, the proposed methods can reduce overfitting on solar cell datasets to increase the prediction performances.

Keywords: Solar cell; Gramian angular field; Recursive plot; Convolutional neural network; Hybrid power generation.
Received: 09 January 2024; Revised: 02 April 2024; Accepted: 31 May 2024.
Article type: Research article.

1. Introduction

The popular world issues include environmental pollution, energy crisis, and global warming. As those matters are getting more attention, renewable energy is considered one of the solutions to the energy crisis.[1] Even dough solar sunlight reaching the earth's surface is thousands of times higher than what humans need now,[2] the conversion efficiency and the usage are still limited. The use of solar energy is not independent of forecasting methods as the availability changes overtime and the resources should adjust themselves accordingly. As proposed in this paper, the use of deep learning algorithms has also been popular research for some time. Recurrent neural network (RNN) and long short-term memory network (LSTM) have been widely used in Ref. [3,4]. Solar cell power can be predicted periodically hourly as in Ref. [5], daily,[6] or for some viewpoints.[7] This paper sought the implementation of solar power prediction to predict the backup power required so that hybrid solar cell–diesel power generation can continuously provide sufficient energy for daylight energy requirements.

As mentioned previously, even though solar power is abundantly available in nature,[8] short-term solar cell output prediction helps energy providers avoid energy shortages by predicting energy injection from other sources.[9] The hybrid solutions may also employ other renewable energy sources such as biomass, micro-hydro, and wind turbines.[8] However, these may generate additional issues. There will be more than one probabilistic-dependent energy source existing. Therefore, this paper chose diesel-generation as the main injector in hybrid power generation as the fuel component determines the output.

Since the availability of solar energy is greatly dependent on solar irradiation and weather,[8] data on irradiation intensity,

[1] *Electrical Engineering Department, Universitas Sumatera Utara, 2 Almamater Road, Medan 20155, Indonesia.*
[2] *Industrial Engineering Department, Universitas Sumatera Utara, 2 Almamater Road, Medan 20155, Indonesia.*
[3] *Information System Department, King Abdulaziz University, Jeddah, 21589, Saudi Arabia.*
**Email:* suherman@usu.ac.id (S. Suherman)

© Engineered Science Publisher LLC 2024

ambient temperature and module temperature becomes the primarily important parameter in prediction.[10] Data recording depends on the locations where the system is implemented. The recorded data is prone to be intermittent, stochastic, and variable.[11] The cloud movement results in stochastic fluctuations. This also led to utilization efficiency, energy balance, and power stability problems. High-accuracy forecasting requires historical meteorological data and recorded electrical properties as training and testing datasets for deep learning models. However, dataset availability is so limited. Furthermore, weather forecasting data is also complicated. So that weather characteristics are limited only to solar cell environments to minimize complications.[12] To manage the prediction of solar cell–diesel hybrid capacity requirement, a solar cell output power pattern is processed using statistical approaches and image transformations before a deep learning algorithm is processed.

Deep learning can be used to predict solar cell output in various time horizons: weekly, daily, hourly, and minutely. Short prediction requires the real-time irradiance mapping model,[13] while long-term forecasts require recorded data.[14] Nelega *et al*. classify time horizon predictions as intra-hour (less than 1 hour), intra-day forecast (1 hour - 6 hours), six hours today ahead (6 hours - 48 hours) and long-term forecasts. The short term is mostly for load prediction, while the long-term is for bigger scenarios such as transmission management, trading, and asset optimizations.[15]

Solar cell prediction may use physical, statistical, and machine learning approaches before using deep learning methods. The physical model uses mathematical equations to derive relationships between the physical state and solar irradiance.[16] The method depends on the climate and the dynamic solar irradiance, which results in a less accurate prediction. Statistical models observe the trend of historical time series and search for the mathematical relationship between historical data and the targeted parameter. Some statistical methods have been used for solar power prediction, such as the autoregressive model,[17] autoregressive moving average (ARMA), autoregressive integrated moving average (ARIMA),[18] seasonal autoregressive integrated moving average (SARIMA),[19] and SARIMA with exogenous factor (SARIMAX).[20] Lastly, machine learning prediction in various applications, including solar cells, depends on the dataset performances and the observed parameters.[21] Some machine learning models, such as extreme learning machines (ELM), are employed.[22] Quantum-based machine learning algorithms have also been involved in many applications, including solar cell prediction.[23]

Artificial neural networks (ANN) are often compared to machine learning and statistical methods in their application in predicting solar cell output. However, the deep neural network has replaced ANN to achieve higher accuracy.[24] Deep learning models such as convolutional neural network (CNN), recurrent neural network (RNN), long-short term memory (LSTM) have been widely used in solar cells.[25] RNN has a feedback connection to the stored information, making it frequently used for periodic data. However, RNN faces problems in long-term time dependencies as the gradient may vanish.[26] LSTM as the extended version of RNN is considered better in handling solar cell data.[27,28] The grid search algorithm for hyperparameter optimization increases prediction performances. Other optimization strategies also help deep learning achieve higher precision, such as multi-input multi-output (MIMO) based optimization strategy.[29] Hyper-parameter optimization based on a tree-structured Parzen Estimator has also been introduced in Ref. [30], which iteratively uses historical parameters to create models. Other advancements in deep learning are also achieved by using hybrid models between machine learning and deep learning, such as GASVM and CNN-LSTM models.[31] Quantum computing was also introduced in deep learning, such as using a hybrid quantum long short-term memory (QLSTM) model, which combined variational quantum computing and LSTM.[32] The study shows that the predicted solar cell output tends to experience overfitting since the power generation pattern is repeated and almost in the same order. As a result, the prediction accuracy on new datasets is worsened. Various techniques have been suggested to reduce overfitting, such as early-stopping, network-reduction, expansion of the training data, and regularization.[33] Those techniques have been evaluated, but they generated similar patterns and did not successfully reduce the overfitting on solar cell datasets. This paper proposes an architecture for hybrid solar cell and diesel power generations and predicts the solar cell output by using folded time-shifted gramian angular field GAF-CNN and recursive plot RP-CNN. Some techniques were also assessed, including multilayer perceptron (MLP), GAF-CNN, RP-CNN with per row data labeling, high-low labeling, and per-day labeling.

2. Experimental and theoretical section

2.1 Hybrid architecture

This paper uses the power generation model, as shown in Fig. 1. The direct (DC) output of the solar cell is stored in the battery through a charger controller converted to alternating (AC) through an inverter. DC voltage ranges from 12 to 48 volts depending on the 12 V battery arrangement and solar panel serial-parallel configurations. The charger controller has

 © Engineered Science Publisher LLC 2024

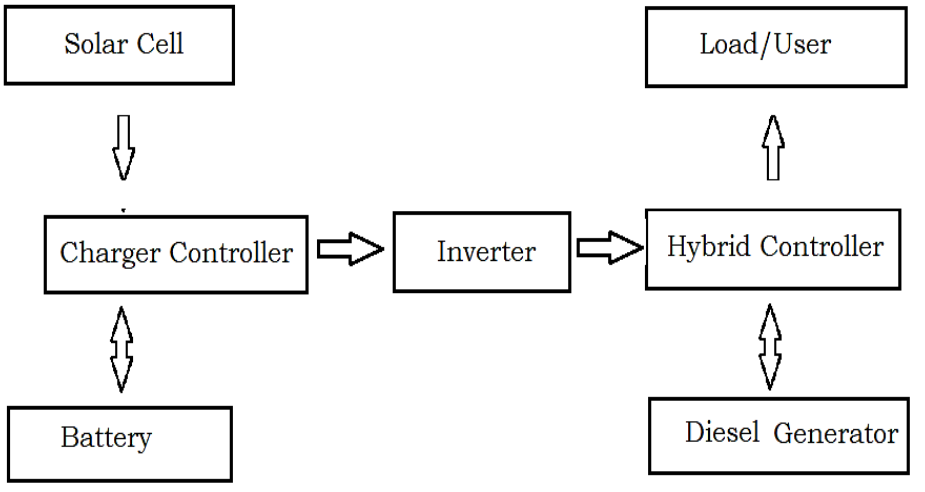

Fig. 1 Hybrid power generation model.

an upper and lower threshold for charging and discharging the battery to expand the battery lifetime. The inverter converts 12 V to 48 V DC voltage to 220 V AC voltage.

The electrical energy demand is fulfilled by combining solar cells and diesel generators. Diesel power generation requires fuel that should be predicted daily. Therefore, predicting the next day's power requirement is important to provide continuous services.

Weather forecasting data, especially temperature, is easily obtained from the weather forecasting department, which is useful for predicting the output power of the solar cell. This is mainly used for energy planning related to hybrid power generation. In the case of the proposed architecture, fuel can be reflected from the predicted solar cell output. If the power demand is denoted as $Demand_{pred}$ and the predicted solar cell output as $Cell_{pred}$ Then, the required diesel power generation is determined using Equation 1. Diesel power prediction and fuel requirement depend on the generator type. However, this will be an easy task once diesel power is predicted.

$$Diesel_{pred} = Demand_{pred} - Cell_{pred} \quad (1)$$

2.2 Folded time-shifted gramian angular field

Since the daily solar cell power generation forms a repeated pattern each day, the daily pattern can be represented as a daily image. Therefore, images are used as input to neural networks. If a time series of X with n components are written as follows: $X = \{x1, x2, \dots, xn\}$, then it can be rescaled to the interval of $[-1, 1]$ resulting in the Equation 2 expression.[34]

$$\tilde{x} = \frac{(xi - \max(X) + (xi - \min(X))}{\max(X) - \min(X)} \quad (2)$$

Equation 2 can be converted into polar coordinates by converting values as angular cosine with radius r, as in Equation 3.[34] The value ti shows the time stamp and the value N is to regularize the span of the polar coordinate system.

$$\emptyset = \arccos(\tilde{x}i), -1 \leq 1, \tilde{x}i \in \tilde{X}$$
$$r = \frac{ti}{N}, ti \in \mathbb{N} \quad (3)$$

As time increases, the corresponding $\emptyset$ and r values are distributed at angular points on the spanning circles. The angular perspective of Equation 3 can be translated into the trigonometric sum as defined in Equation 4.[34]

$$G = \begin{bmatrix} \cos(\emptyset 1 + \emptyset 1) & \cdots & \cos(\emptyset 1 + \emptyset n) \\ \cos(\emptyset 2 + \emptyset 1) & \dots & \cos(\emptyset 2 + \emptyset n) \\ \vdots & \ddots & \vdots \\ \cos(\emptyset n + \emptyset 1) & \dots & \cos(\emptyset n + \emptyset n) \end{bmatrix} \quad (4)$$

G is called as a Gramian matrix. By defining the inner product of $< x, y >= x.y - \sqrt{1-x^2}.\sqrt{1-y^2}$, Gramian matrix G can be expressed as Equation 5 [34].

$$G = \begin{bmatrix} < \tilde{x}1, \tilde{x}1 > & \cdots & < \tilde{x}1, \tilde{x}n > \\ < \tilde{x}2, \tilde{x}1 > & \dots & < \tilde{x}2, \tilde{x}n > \\ \vdots & \ddots & \vdots \\ < \tilde{x}n, \tilde{x}1 > & \dots & < \tilde{x}n, \tilde{x}n > \end{bmatrix} \quad (5)$$

The data series is transformed into matrix data as the CNN input maintains the raw time series data.[35] Some works have implemented GAF with multiscale CNN, fully convolutional network, GAF-MTF, recursive plot (RP)[36-38] and RPCNN. In GAF-MTF, MTF calculates the probability of transition using the Markov chain. The RP-based representation uses 2-D images to locate the position at which data tends to revert to a prior state. However, RP is sometimes imbalanced on the common datasets. ConvNet defined gramian angular summation field (GASF), gramian angular difference field (GADF), and MTF where images are combined by using RGB channels.[39] Google popularized the micro-moments GAF (M2GAF) and is mature enough to encapsulate energy data and contextual ambient conditions.Qu *et al*. constructed the

© Engineered Science Publisher LLC 2024

weighted voltage–current (WVI) trajectory, MTF, and current spectral sequence-based GAF (I-GAF) images, and CNN with energy-normalization and squeeze-and-excitation blocks (EN-SE-RECNN) for electrical appliance recognition.[40] Chen *et al* used three single-channel GAF images within three channels RGB for load signatures.[41] Zhang *et al*. proposed learnable recurrent graph (LRG), learnable Gramian matrix (LGM), and generative graph (GG) for learnable process. More research can be found regarding GAF development.[42]

This research proposes the folded time-shifted gramian angular field and recursive plot to reduce the overfitted data. The proposed method to reduce overfitting in solar cell power prediction is performed by applying two techniques. At the initial stage, a folded image for one day of data is performed. Assume that an image is converted from the series in Equation 6.

$$Y_t = a_o x_o + a_1 x_1 + \ldots + a_{t-1} x_{t-1} \quad (6)$$

This data is then folded into Equation 7 and Equation 8.

$$Y_t^0 = a_o x_o + a_1 x_1 + \ldots + a_{t-1} x_{t/2-1} \quad (7)$$

$$Y_t^1 = a_{t-1} x_{t-1} + a_{t-2} x_{t-2} + \ldots + a_{t/2} x_{t/2} \quad (8)$$

The next step is shifting the time of neighboring components with differences less than a certain threshold. If the difference is less than the threshold, this value will be omitted and converted to zero. Otherwise, the value remains similar. This shifting will add variations to the dataset. The process is modeled by Equation 9.

$$a_i x_i = \begin{cases} 0 \; if \; abs\{a_i x_i - a_{i+1} x_{i+1}\} < threshold, for \; i = 1, 3, 5 \ldots \\ a_i x_i \; if \; abs\{a_i x_i - a_{i+1} x_{i+1}\} > threshold, for \; i = 1, 3, 5 \ldots \end{cases} \quad (9)$$

The illustration is shown in Fig. 2.

2.3 The experimental setup

Research steps are illustrated in a flowchart, as shown in Fig. 3. The initial step is choosing and cleaning the datasets. The statistical parameter is then assessed. The possible transformation dataset to get a better distribution may be applied afterward. The dataset is then modified to satisfy training and test requirements. The next step is to analyze the prediction performance, which involves deep learning execution, variations, modification, repeated experiments and performance plotting. The plotted electricity demand was assumed to be known, so the analysis focuses on solar power prediction. If these two parameters are known, the required power for a diesel generator can be calculated, and fuel prediction can be performed. Solar cell data should provide enough number of evaluated days so that patterns are sufficient.

Data was taken and cleaned from GitHub repositories.[42] Samples are presented in Table 1. Data comprises 578 days of recordings from Nov 11, 2015, to Oct 31, 2017, 54 slot time every day, recorded every 10 minutes from 8.30 AM to 5.20 PM. The dataset period has no impact on analysis as data is compared to its label. The expected data is often non-normally distributed, which makes prediction more difficult. Therefore, statistical data analysis is performed to obtain a better distribution. First, difference and fractional difference are applied to get a better distribution. Table 2 shows the properties of the original dataset. There are 30839 rows with a mean of 431.566, with skewness of 1.0195 and kurtosis of -0.13. Data is not symmetric and is not normally distributed. The obtained datasets have distribution, correlation, and solar power samples, as shown in Fig. 4. It is clearly demonstrated that dataset distribution is not normally distributed. Neighboring data is too close as autocorrelation smoothly decreases, and the pattern is repeated daily. This is the biggest challenge, as the data is potentially overfitted. Data transformation is performed to enhance predictivity.

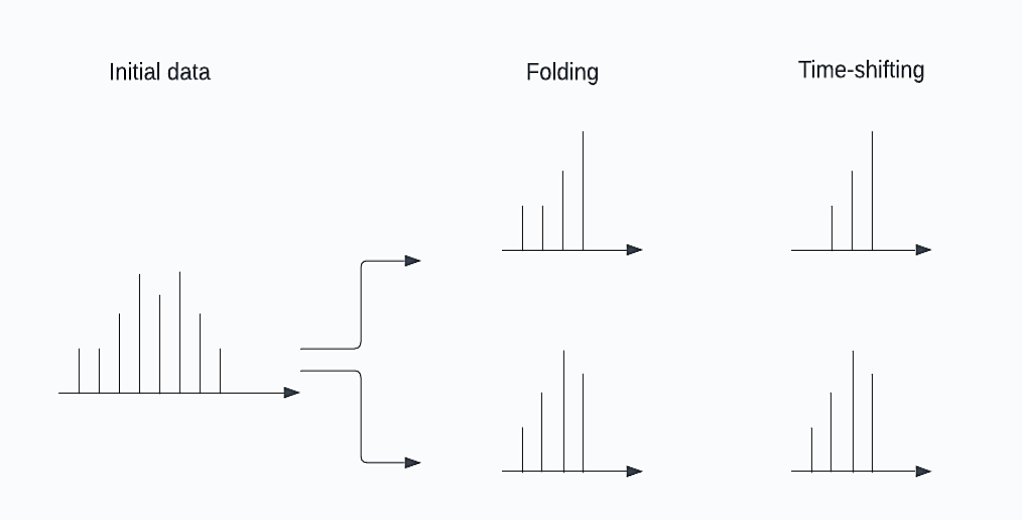

Fig. 2 Folded time-shifted method.

© Engineered Science Publisher LLC 2024

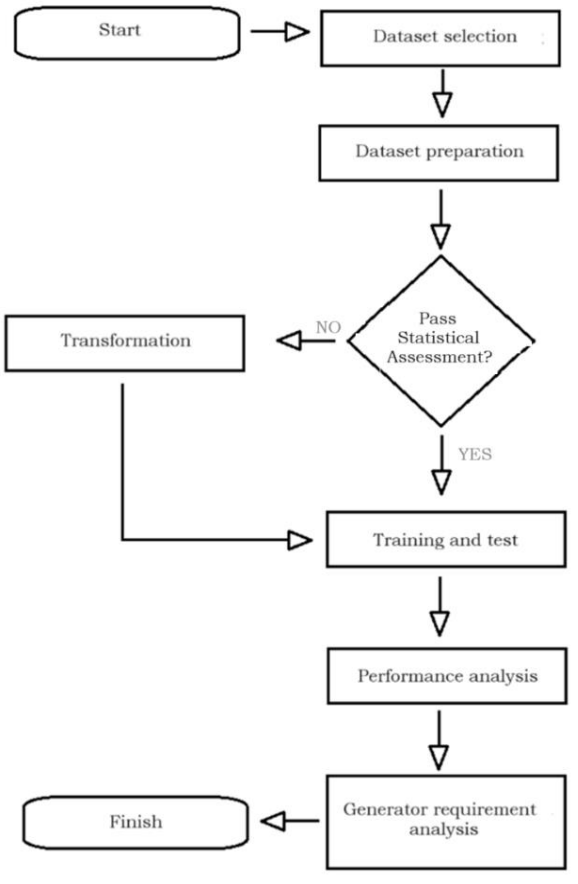

Fig. 3 Research steps.

Table 1. Solar cell power generation.

SEQ	Date	Time	Temp (°C)	Power (W)
1	11/11/2015	8:30:00 AM	17.9	0
1	11/11/2015	8:40:00 AM	18.1	0
2	11/11/2015	8:50:00 AM	18.3	0
3	11/11/2015	9:00:00 AM	18.7	19
4	11/11/2015	9:10:00 AM	19.2	33
…..	…..	…..	…..	…..
30834	10/31/2017	4:40:00 PM	23.2	31
30835	10/31/2017	4:50:00 PM	23.0	26
30835	10/31/2017	5:00:00 PM	22.8	15
30835	10/31/2017	5:10:00 PM	22.4	6
30835	10/31/2017	5:20:00 PM	22.1	2

Table 2. Dataset statistics.

Parameter	Value
count	30839
mean (W)	431.566069
std (W)	401.412382
min (W)	0
25% (W)	118
50% (W)	276
75% (W)	663
Max (W)	1654
Skewness:	1.019545109
Kurtosis:	-0.13590065

Transformation can be performed through normalization, regularization, and data selection on power, voltage, current, or other physical measure. Transformation can also be performed by choosing the correct labeling. This paper uses three approaches regarding labeling.

3. Results and discussions

Three approaches were used to define the dataset label to fit the requirements for predicting power. Since solar power is available only during days and the quantity was assumed insufficient to serve customer demand, diesel fuel should be projected to drive the generator during daylight. Dataset labels were designed to satisfy neural network processing as follows: Power prediction is used for dataset labels per row (per row labeling). Since datasets were taken every 10 minutes, power data is used as prediction labels per row as real generated power. This paper uses statistical approaches to dataset distribution and applies MLP for prediction. Power predictions are made as an increase or a decrease (high and low labeling). If the power in the current row of datasets is higher than that of the previous row, the label is set to high or "true". Otherwise, it is low or "false." This paper applies GAF-CNN and RP-CNN for this step. Power predictions use power data as the sum of daily generation (per day labeling). This paper uses GAF-CNN, RP-CNN, and the proposed technique for this step.

3.1 Per row labeling

This article uses original data, first difference, and fractional difference datasets. Fig. 5a shows initial statistical data. Figs. 5b and 5c show the first and fractional difference statistical data. The first difference is an ordinary least square (OLS) estimation obtained by taking the first differences over the dataset.[43] If Yt is the dataset, then the first difference is $Y_t - Y_{t-1}$. While fractional differences involve probability d and are modeled as:

$$Y_t = dY_t^1 + (1-d)Y_t^0 \quad (10)$$

The MLP implementation uses the MLP Regressor Python library with a number of hidden layer sizes of 150. The activation method uses relu and adam as the optimizer, as shown in Fig. 6a. For training data, the first difference transformation has the highest R2 score of 0.832. In comparison, the test dataset is 0.35. However, overfitting is still an issue because test data is much lower than training data. On the other hand, original data and fractional difference data make MLP produce a negative R2 score for test data, which means that data is heavily overfitting. This shows that the method still produces bad performances. The correlation between predicted and real data is even worse, as shown in Fig. 6b.

© Engineered Science Publisher LLC 2024

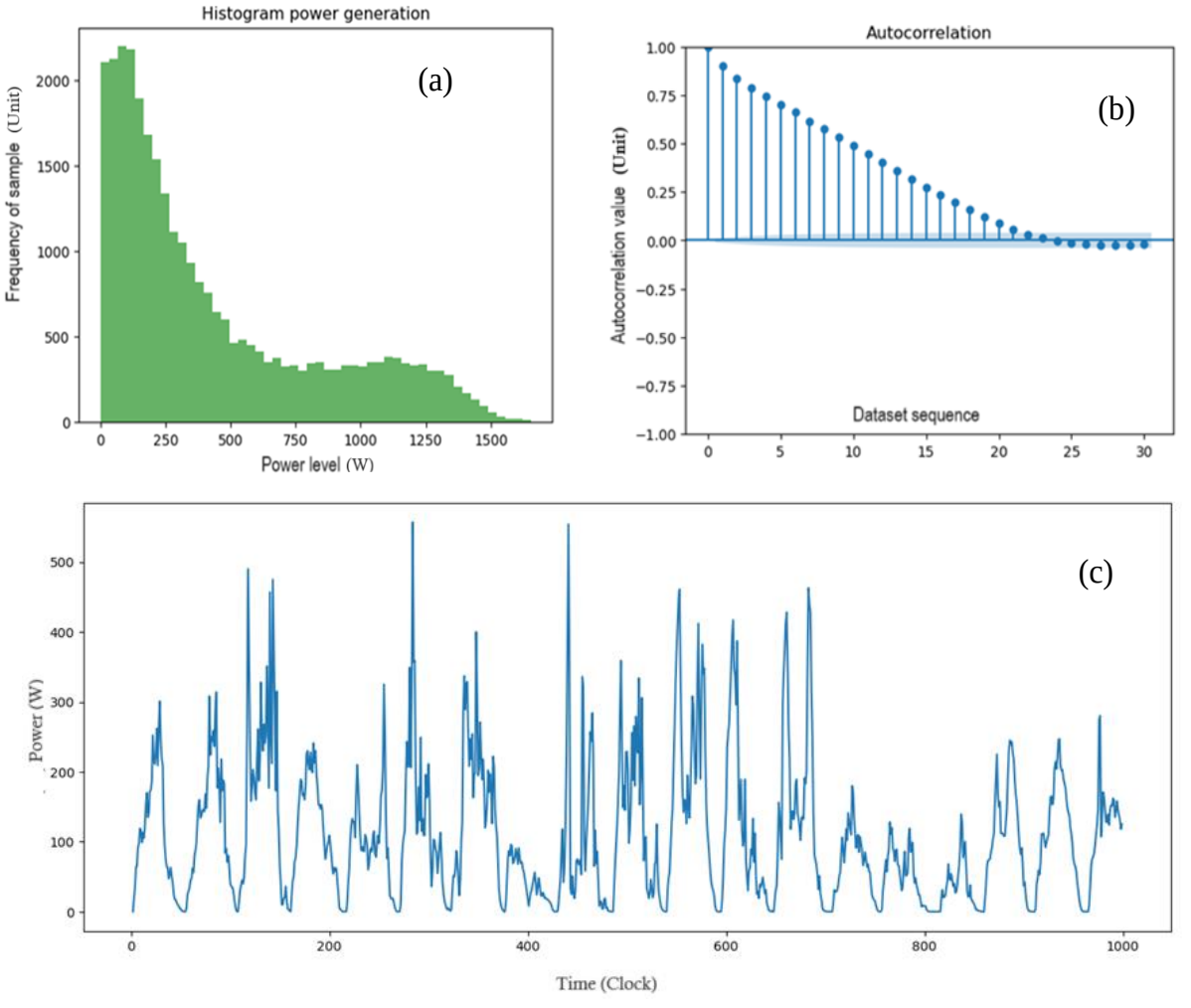

Fig. 4 Statistic properties of dataset: (a) The non-normally data distribution; (b) Autocorrelation with smooth changes; (c) Data variations.

3.2 High and low labeling

The GAF-CNN and RP-CNN are employed for power labeling generated into two classes: higher (true), which means that tomorrow's power prediction is higher than today's prediction; lower (false), which means that the tomorrow's power production is lower than of today. The temperature data as the feature data is converted to an image series using GAF, as depicted in Fig. 7. The true and false labels are contained in an array as data labels per row. Since data from 08.30 AM to 105.20 PM includes 54 columns, the image is resized to 54×54 resolution.

Unfortunately, the result shows that the training data is overfitting, which causes training data to have accuracy reaching 91.2%, while test data accuracy decreases to less than 40%. The plot is shown in Fig. 8. Further adjustment is performed by decreasing the number of nodes and layers and applying early stopping and regularization. However, the results are not far from the plotted performances.

3.3 Per day labelling

This paper then classified the generated power into five classes: 0 (0-10000 power unit), 1 (10000-20000 power unit) , 2 (20000-30000 power unit), 3 (30000-40000 power unit), and 5 (40000-50000 power unit). The data is then trained and tested by using both GAP-CNN and RP-CNN. Fig. 9 shows that the data is still overfitted.

3.4 The proposed method

The proposed methods produce additional dataset lines. The first line contains features from 08.30 AM to 12.00 AM, the second line is data from 00.10 PM to 05.20 PM as the folded components, and the third one is the shifted components. These additional lines help the model to predict various conditions. As a result, the overfitting phenomenon can be minimized by reducing losses and increasing accuracy for testing data. The dataset's composition is better than the datasets achieved by transformation. The prediction performance also gets better. The proposed techniques are applied to GAF-CNN and RP-CNN. Fig. 10 shows the performance improvements.

© Engineered Science Publisher LLC 2024

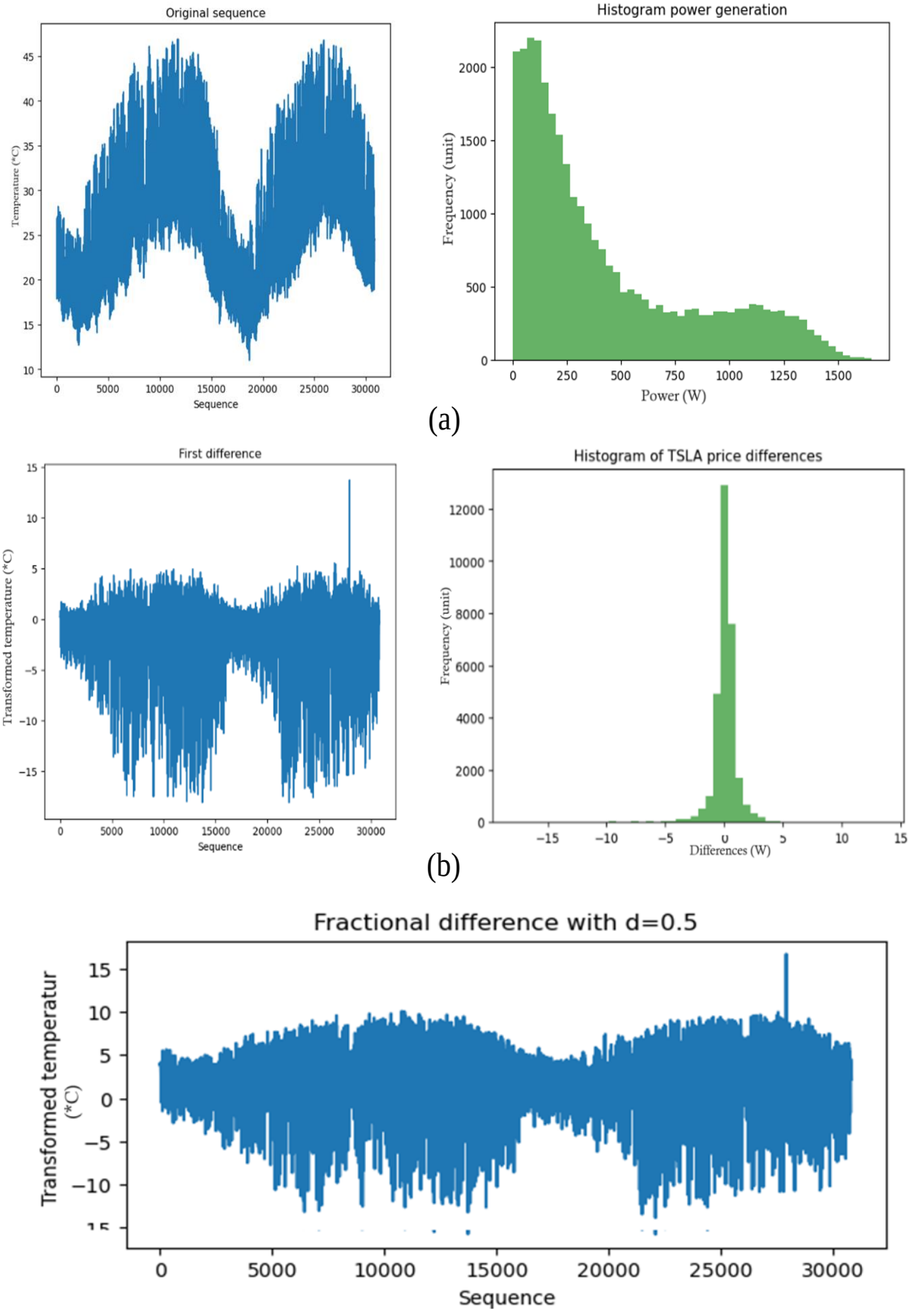

Fig. 5 Dataset transformations: (a) original data with non-normal distribution; (b) First difference with normal distribution; (c) Fractional differences plot.

© Engineered Science Publisher LLC 2024

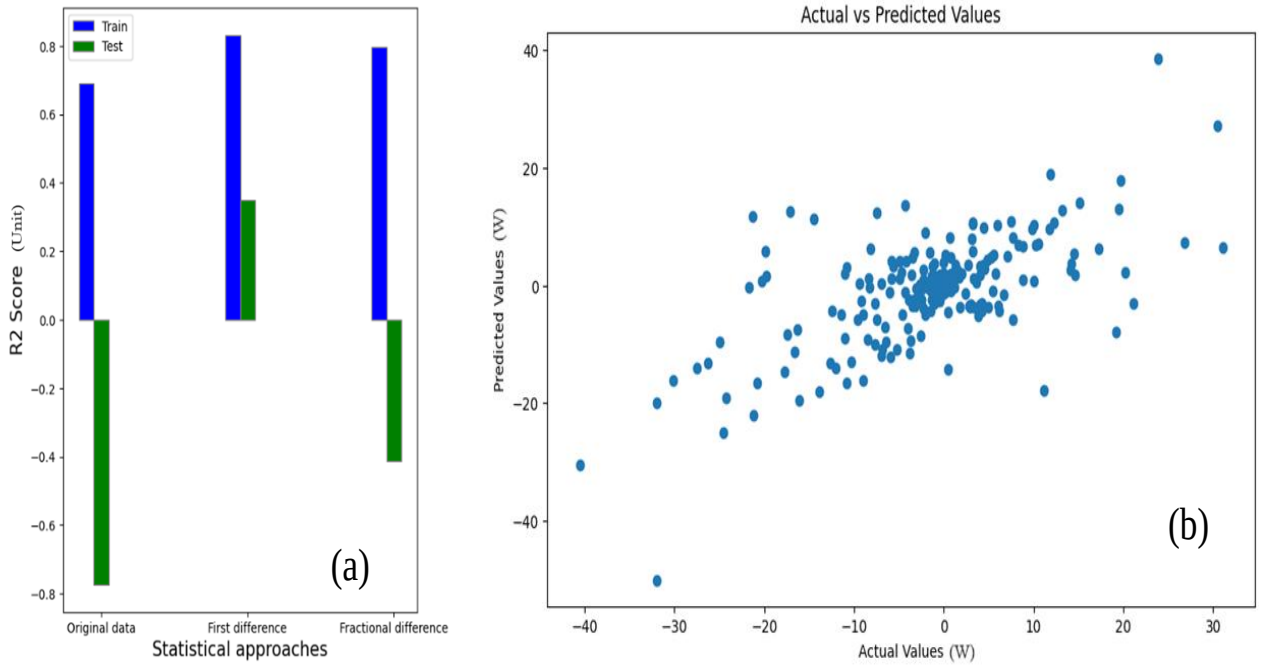

Fig. 6 MLP performance: (a) R2 score; and (b) Prediction distribution.

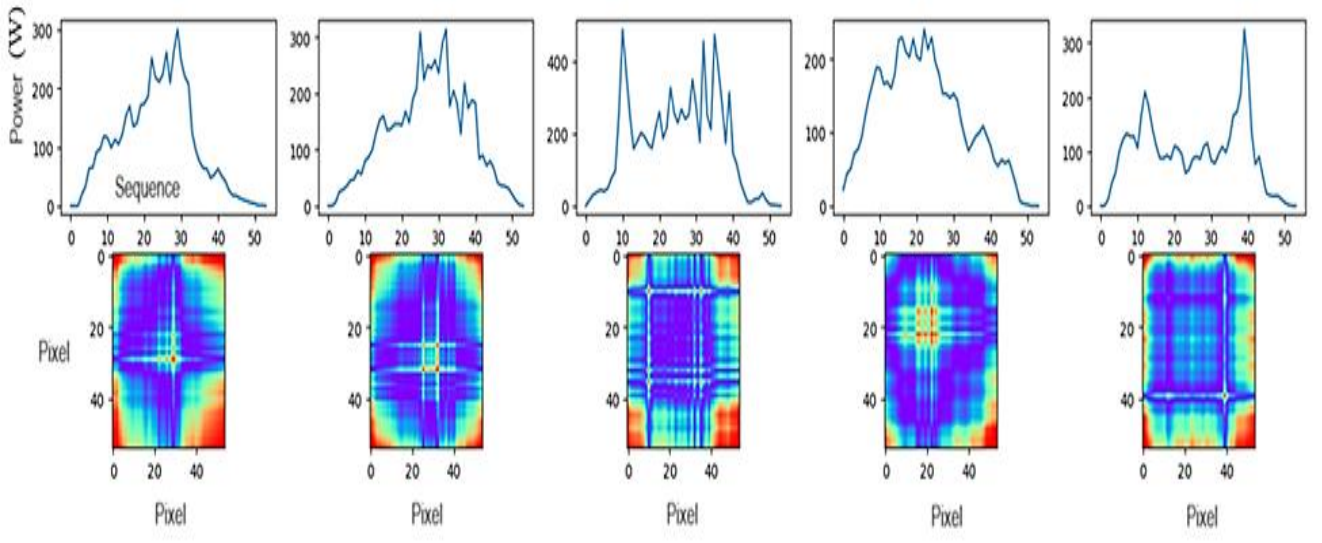

Fig. 7 Six samples of image conversions on datasets.

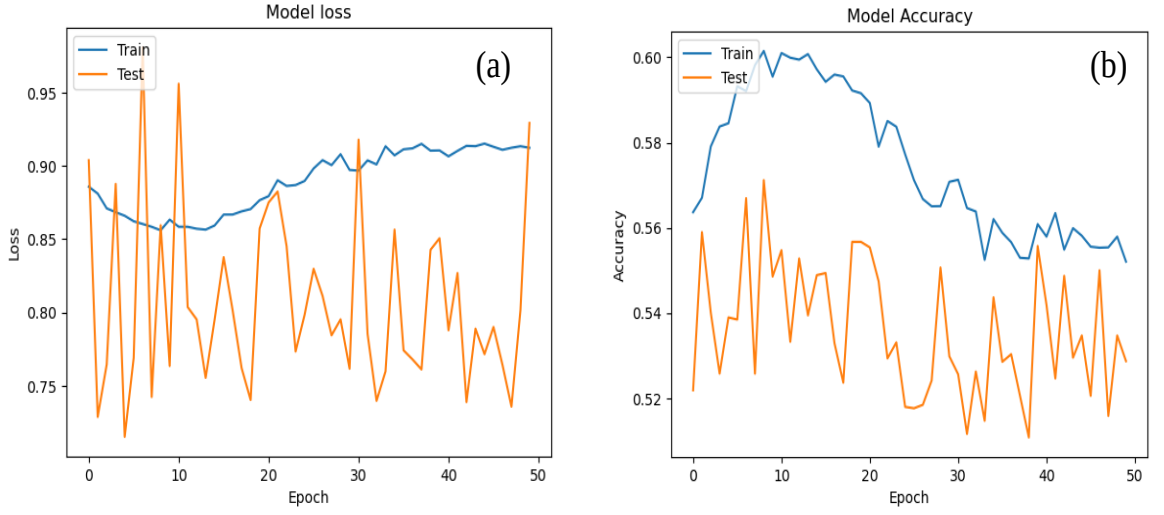

Fig. 8 High-low labeling performance: (a) Loss and (b) Accuracy for various epochs.

© Engineered Science Publisher LLC 2024

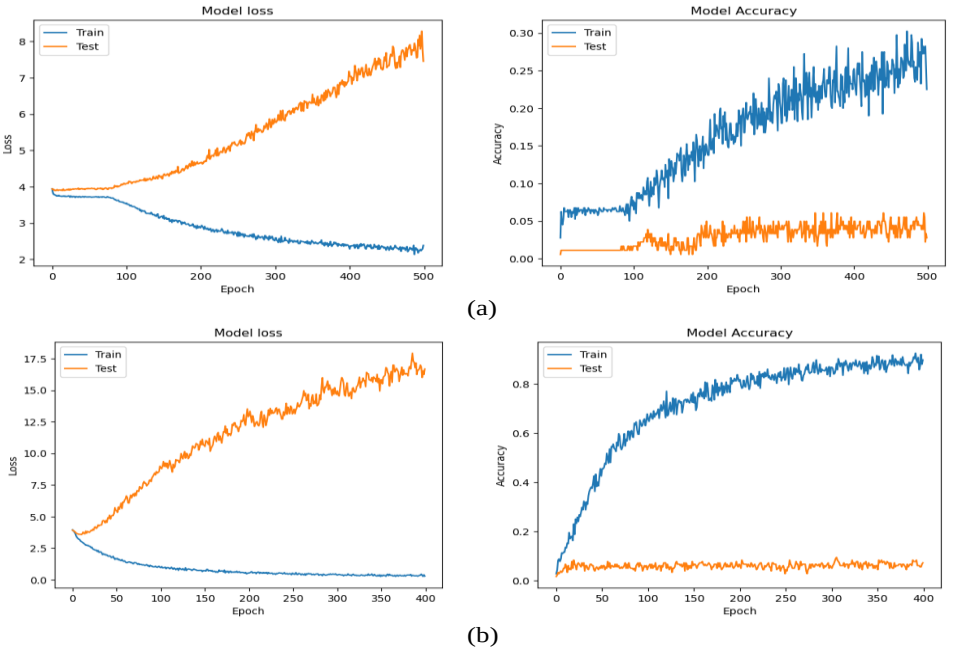

Fig. 9 Per-day labelling performance: (a) Using GAF-CNN; (b) Using RP-CNN performances.

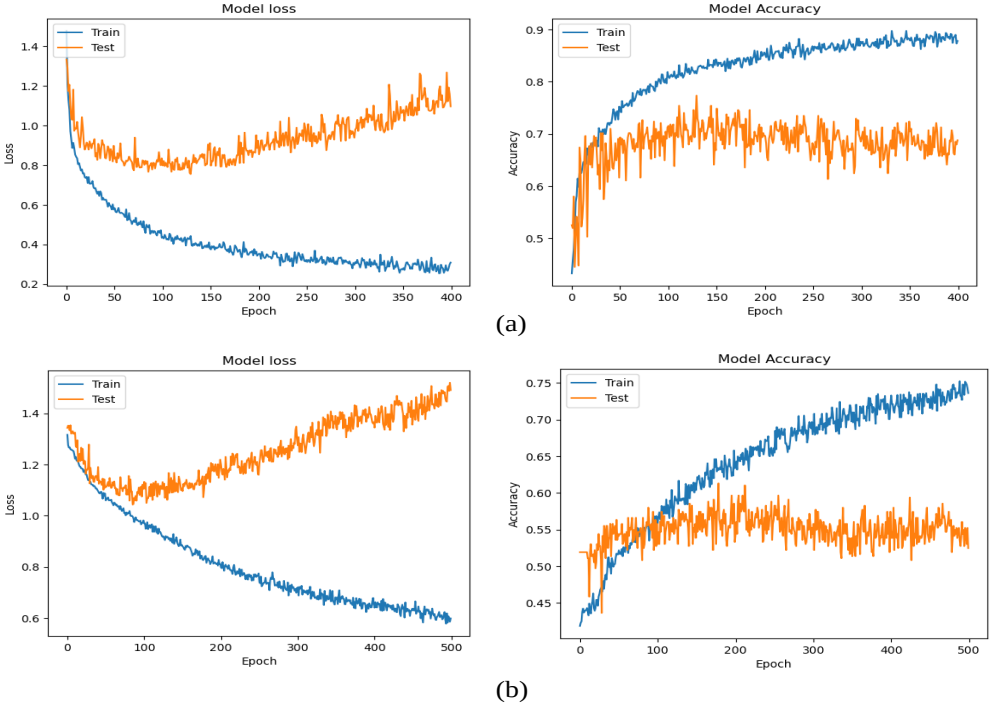

Fig. 10 The proposed folded and time-shifted performances: (a) Folded Time-shifted GAF-CNN; (b) Folded Time-shifted RP-CNN.

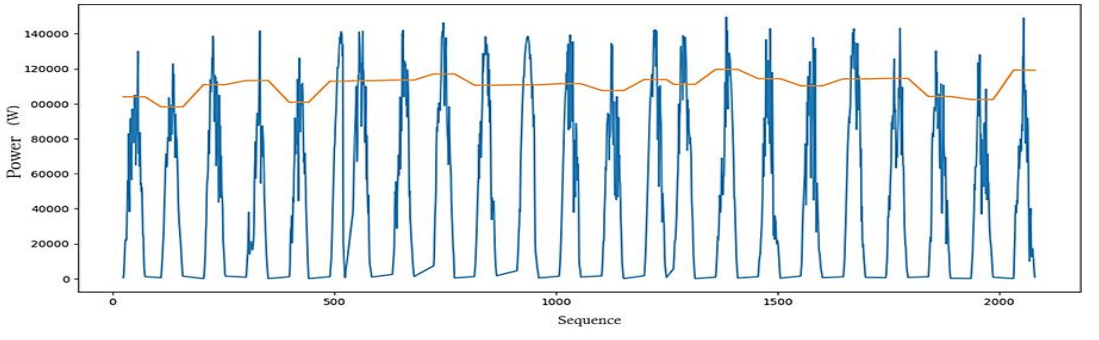

Fig. 11 Power demand and solar cell capabilities.

© Engineered Science Publisher LLC 2024

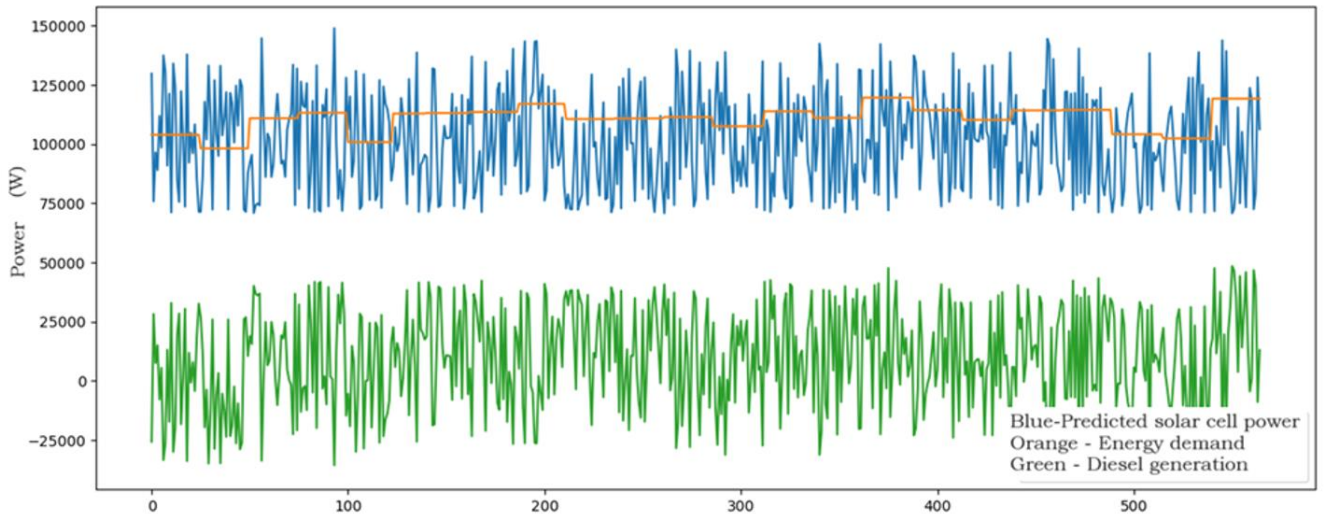

Fig. 12 Diesel power prediction.

3.5 Diesel generator energy calculation

When the demand for electricity and the predicted solar cell output have been analyzed, the expected power from the diesel generator can be calculated. The more accurate the solar power prediction, the more accurate the diesel power calculation. If it is assumed that energy demand achieves 80% of the maximum solar cell output, the sample of the power plot is illustrated in Fig. 11. The yellow line shows the demand. Solar cells can only provide requirements fully when solar cell output is at its peak. But diesel generators fill the gap because solar power is lower than its peak.

Diesel power requirement is obtained from the demand and the predicted solar power differences. A sample of calculations is shown in Fig. 12. Generator fuel calculation depends on generator specification, as each generator type has a different fuel-energy mapping.

4. Conclusions

This paper has examined solar cell datasets, applying various approaches to make prediction possible for hybrid solar cell and diesel power generations. Dataset applications make use of various labeling approaches, including per-row data assessment, high-low power generation and per-day power generation. Multilayer perceptron, GAF-CNN and RP-CNN were employed, as well as regularization and drop-out. However, even though several efforts had been tried, datasets remained overfitted, represented by high accuracy for training data but low accuracy for test data. The proposed folded technique divided data into up and down parts, separating increasing and decreasing solar power during morning and afternoon. After that, neighboring data with almost similar values is then shifted, resulting in zero for one of them. Applying this approach to GAF-CNN and RP-CNN reduced the overfitting phenomenon significantly. Next-day power generation can be predicted more concisely using this proposed technique so that the required diesel power can be predicted.

For future work, it is recommended that further modifications and combinations are performed for both data transformations and image analysis techniques before CNN processing. In addition, some periods of data samples have rapid changes in measured power. Others have slower variations. These conditions can be taken into consideration for further partial dataset adjustment to reduce overfittness.

Acknowledgments

This research has been supported by Universitas Sumatera Utara, Medan City - Indonesia.

Conflict of Interest

There is no conflict of interest.

Supporting Information

Not applicable.

References

[1] C. Breyer, S. Khalili, D. Bogdanov, M. Ram, A. S. Oyewo, A. Aghahosseini, A. Gulagi, A. A. Solomon, D. Keiner, G. Lopez, P. A. Ostergaard, H. Lund, B. V. Mathiesen, M. Z. Jacobson, M. Victoria, S. Teske, T. Pregger, V. Fthenakis, M. Raugei, H. Holttinen, U. Bardi, A. Hoekstra, B. K. Sovacool, On the history and future of 100% renewable energy systems research, *IEEE Access*, 2022, **10**, 78176-78218, doi: 10.1109/access.2022.3193402.

[2] A. Pandey, P. Pandey, J. S. Tumuluru, Solar energy production in India and commonly used technologies—an overview, *Energies*, 2022, **15**, 500, doi: 10.3390/en15020500.

 © Engineered Science Publisher LLC 2024

[3] M. Abdel-Nasser, K. Mahmoud, Accurate photovoltaic power forecasting models using deep LSTM-RNN, *Neural Computing and Applications*, 2019, **31**, 2727-2740, doi: 10.1007/s00521-017-3225-z.
[4] M. K. Park, J. M. Lee, W. H. Kang, J. M. Choi, K. H. Lee, Predictive model for PV power generation using RNN (LSTM), *Journal of Mechanical Science and Technology*, 2021, **35**, 795-803, doi: 10.1007/s12206-021-0140-0.
[5] M. N. Akhter, S. Mekhilef, H. Mokhlis, Z. M. Almohaimeed, M. A. Muhammad, A. S. M. Khairuddin, R. Akram, M. M. Hussain, An hour-ahead PV power forecasting method based on an RNN-LSTM model for three different PV plants, *Energies*, 2022, **15**, 2243, doi: 10.3390/en15062243.
[6] F. Harrou, F. Kadri, Y. Sun, Forecasting of photovoltaic solar power production using LSTM approach, *Advanced Statistical Modeling, Forecasting, and Fault Detection in Renewable Energy Systems*, 2020, doi: 10.5772/intechopen.91248.
[7] Y.-K. Wu, C.-L. Huang, Q.-T. Phan, Y.-Y. Li, Completed review of various solar power forecasting techniques considering different viewpoints, *Energies*, 2022, **15**, 3320, doi: 10.3390/en15093320.
[8] M. N. Akhter, S. Mekhilef, H. Mokhlis, N. Mohamed Shah, Review on forecasting of photovoltaic power generation based on machine learning and metaheuristic techniques, *IET Renewable Power Generation*, 2019, **13**, 1009-1023, doi: 10.1049/iet-rpg.2018.5649.
[9] W. VanDeventer, E. Jamei, G. S. Thirunavukkarasu, M. Seyedmahmoudian, T. K. Soon, B. Horan, S. Mekhilef, A. Stojcevski, Short-term PV power forecasting using hybrid GASVM technique, *Renewable Energy*, 2019, **140**, 367-379, doi: 10.1016/j.renene.2019.02.087.
[10] C. N. Obiora, A. Ali, A. N. Hasan, Estimation of hourly global solar radiation using deep learning algorithms, 2020 11th International Renewable Energy Congress (IREC), 2020.
[11] F. Wang, Z. Xuan, Z. Zhen, K. Li, T. Wang, M. Shi, A day-ahead PV power forecasting method based on LSTM-RNN model and time correlation modification under partial daily pattern prediction framework, *Energy Conversion and Management*, 2020, **212**, 112766, doi: 10.1016/j.enconman.2020.112766.
[12] D. Yang, W. Li, G. M. Yagli, D. Srinivasan, Operational solar forecasting for grid integration: standards, challenges, and outlook, *Solar Energy*, 2021, **224**, 930-937, doi: 10.1016/j.solener.2021.04.002.
[13] F. Wang, Z. Xuan, Z. Zhen, Y. Li, K. Li, L. Zhao, M. Shafie-khah, J. P. S. Catalão, A minutely solar irradiance forecasting method based on real-time sky image-irradiance mapping model, *Energy Conversion and Management*, 2020, **220**, 113075, doi: 10.1016/j.enconman.2020.113075.
[14] J. J. Mesa-Jiménez, A. L. Tzianoumis, L. Stokes, Q. Yang, V. N. Livina, Long-term wind and solar energy generation forecasts, and optimisation of Power Purchase Agreements, *Energy Reports*, 2023, **9**, 292-302, doi: 10.1016/j.egyr.2022.11.175.
[15] R. Nelega, D. I. Greu, E. Jecan, V. Rednic, C. Zamfirescu, E. Puschita, R. V. F. Turcu, Prediction of power generation of a photovoltaic power plant based on neural networks, *IEEE Access*, 2023, **11**, 20713-20724, doi: 10.1109/ACCESS.2023.3249484.
[16] Y. Hao, C. Tian, A novel two-stage forecasting model based on error factor and ensemble method for multi-step wind power forecasting, *Applied Energy*, 2019, **238**, 368-383, doi: 10.1016/j.apenergy.2019.01.063.
[17] M. López, C. Sans, S. Valero, C. Senabre, Empirical comparison of neural network and auto-regressive models in short-term load forecasting, *Energies*, 2018, **11**, 2080, doi: 10.3390/en11082080.
[18] Aasim, S. N. Singh, A. Mohapatra, Repeated wavelet transform based ARIMA model for very short-term wind speed forecasting, *Renewable Energy*, 2019, **136**, 758-768, doi: 10.1016/j.renene.2019.01.031.
[19] M. H. Alsharif, M. K. Younes, J. Kim, Time series ARIMA model for prediction of daily and monthly average global solar radiation: the case study of Seoul, South Korea, *Symmetry*, 2019, **11**, 240, doi: 10.3390/sym11020240.
[20] G.-C. Lee, S.-H. Choi, Forecasting Foreign Visitors using SARIMAX Models with the Exogenous Variable of Demand Decrease, *Journal of Society of Korea Industrial and Systems Engineering*, 2020, **43**, 59-66, doi: 10.11627/jkise.2020.43.4.059.
[21] G. Narvaez, L. F. Giraldo, M. Bressan, A. Pantoja, Machine learning for site-adaptation and solar radiation forecasting, *Renewable Energy*, 2021, **167**, 333-342, doi: 10.1016/j.renene.2020.11.089.
[22] D. El Bourakadi, H. Ramadan, A. Yahyaouy, J. Boumhidi, A novel solar power prediction model based on stacked BiLSTM deep learning and improved extreme learning machine, *International Journal of Information Technology*, 2023, **15**, 587-594, doi: 10.1007/s41870-022-01118-1.
[23] A. Giani, Z. Eldredge, Quantum computing opportunities in renewable energy, *SN Computer Science*, 2021, **2**, 393, doi: 10.1007/s42979-021-00786-3.
[24] A. Khosravi, R. N. N. Koury, L. Machado, J. J. G. Pabon, Prediction of hourly solar radiation in Abu Musa Island using machine learning algorithms, *Journal of Cleaner Production*, 2018, **176**, 63-75, doi: 10.1016/j.jclepro.2017.12.065.
[25] M. Sabri, M. El Hassouni, Predicting photovoltaic power generation using double-layer bidirectional long short-term memory-convolutional network, *International Journal of Energy and Environmental Engineering*, 2023, **14**, 497-510, doi: 10.1007/s40095-022-00530-4.
[26] H. Hewamalage, C. Bergmeir, K. Bandara, Recurrent Neural Networks for Time Series Forecasting: current status and future directions, *International Journal of Forecasting*, 2021, **37**, 388-427, doi: 10.1016/j.ijforecast.2020.06.008.
[27] M. Abdel-Nasser, K. Mahmoud, Accurate photovoltaic power forecasting models using deep LSTM-RNN, *Neural Computing and Applications*, 2019, **31**, 2727-2740, doi: 10.1007/s00521-017-3225-z.

© Engineered Science Publisher LLC 2024

[28] M. K. Park, J. M. Lee, W. H. Kang, J. M. Choi, K. H. Lee, Predictive model for PV power generation using RNN (LSTM), *Journal of Mechanical Science and Technology*, 2021, **35**, 795-803, doi: 10.1007/s12206-021-0140-0.
[29] D. Sahoo, N. Sood, U. Rani, G. Abraham, V. Dutt, A. D. Dileep, Comparative analysis of multi-step time-series forecasting for network load dataset, 2020 11th International Conference on Computing, Communication and Networking Technologies (ICCCNT), 2020.
[30] H.-P. Nguyen, J. Liu, E. Zio, A long-term prediction approach based on long short-term memory neural networks with automatic parameter optimization by Tree-structured Parzen Estimator and applied to time-series data of NPP steam generators, *Applied Soft Computing*, 2020, **89**, 106116, doi: 10.1016/j.asoc.2020.106116.
[31] W. VanDeventer, E. Jamei, G. S. Thirunavukkarasu, M. Seyedmahmoudian, T. K. Soon, B. Horan, S. Mekhilef, A. Stojcevski, Short-term PV power forecasting using hybrid GASVM technique, *Renewable Energy*, 2019, **140**, 367-379, doi: 10.1016/j.renene.2019.02.087.
[32] Y. Yu, G. Hu, C. Liu, J. Xiong, Z. Wu, Prediction of solar irradiance one hour ahead based on quantum long short-term memory network, *IEEE Transactions on Quantum Engineering*, 2023, **4**, 3100815, doi: 10.1109/TQE.2023.3271362.
[33] H. K. Dishar, L. A. Muhammed, A review of the overfitting problem in convolution neural network and remedy approaches, *Journal of Al-Qadisiyah for Computer Science and Mathematics*, 2023, **15**, 155–165, doi: 10.29304/jqcm.2023.15.2.1240.
[34] A. Al Safi, C. Beyer, V. Unnikrishnan, M. Spiliopoulou, Multivariate time series as images: Imputation using convolutional denoising autoencoder, Advances in Intelligent Data Analysis XVIII: 18th International Symposium on Intelligent Data Analysis, 2020.
[35] J.-H. Choi, J.-S. Lee, EmbraceNet: A robust deep learning architecture for multimodal classification, *Information Fusion*, 2019, **51**, 259-270, doi: 10.1016/j.inffus.2019.02.010.
[36] T. Maria Mihaela,Gerasimos Spanakis, Hybrid Tiled Convolutional Neural Networks (HTCNN) Text Sentiment Classification, ICAART (2), 2020.
[37] S. A. A. Ojeda, E. C. Peramo, G. A. Solano, Application of deep learning in recurrence plots for multivariate nonlinear time series forecasting. Tsihrintzis GA, Virvou M, Jain LC, Advances in Machine Learning/Deep Learning-based Technologies. *Cham: Springer*, 2022, **2**, 169-185, doi: 10.1007/978-3-030-76794-5_9.
[38] C.-L. Yang, Z.-X. Chen, C.-Y. Yang, Sensor classification using convolutional neural network by encoding multivariate time series as two-dimensional colored images, *Sensors*, 2019, **20**, 168, doi: 10.3390/s20010168.
[39] A. Amira, H. Malekmohamadi, K. Diao, F. Bensaali, Elevating energy data analysis with M2GAF: micro-moment driven Gramian angular field visualizations, International Conference on Applied Energy, 2021.
[40] L. Qu, Y. Kong, M. Li, W. Dong, F. Zhang, H. Zou, A residual convolutional neural network with multi-block for appliance recognition in non-intrusive load identification, *Energy and Buildings*, 2023, **281**, 112749, doi: 10.1016/j.enbuild.2022.112749.
[41] J. Chen, X. Wang, Non-intrusive load monitoring using gramian angular field color encoding in edge computing, *Chinese Journal of Electronics*, 2022, **31**, 595-603, doi: 10.1049/cje.2020.00.268.
[42] Y. Zhang, H. Wu, Q. Ma, Q. Yang, Y. Wang, A learnable image-based load signature construction approach in NILM for appliances identification, *IEEE Transactions on Smart Grid*, 2023, **14**, 3841-3849, doi: 10.1109/TSG.2023.3239598.
[43] M. A. Ansari, M. R. Ahmad, S. Siddique, K. Mansoor, An environment Kuznets curve for ecological footprint: evidence from GCC countries, *Carbon Management*, 2020, **11**, 355-368, doi: 10.1080/17583004.2020.1790242.

Publisher's Note: Engineered Science Publisher remains neutral with regard to jurisdictional claims in published maps and institutional affiliations.

 © Engineered Science Publisher LLC 2024